

Probing the structural and topological requirements for CCR2 antagonism: Holographic QSAR for indolopiperidine derivatives

K. Srikanth, Pramod C. Nair and M. Elizabeth Sobhia*

*Centre for Pharmacoinformatics, National Institute of Pharmaceutical Education and Research (NIPER),
Sector 67, S.A.S. Nagar, Punjab 160062, India*

Received 12 September 2007; revised 12 December 2007; accepted 28 December 2007

Available online 1 January 2008

Abstract—CCR2 is the major family of chemokine receptors which involve in the pathophysiology of the acute or chronic inflammatory conditions such as rheumatoid arthritis, atherosclerosis, asthma, obesity, and type-2 diabetes. Herein, we report the results of HQSAR model, developed for CCR2 antagonistic activity of indolopiperidine derivatives. The best HQSAR model with $r^2 = 0.916$, $q^2 = 0.562$ with atom count = 4–7 was used to predict the activity of the test set molecules. The predicted values are in good agreement with experimental results and show the potential of the model for untested compounds. Analysis of molecular fragments throws light on essential structural and topological features of indolopiperidine derivatives for antagonist activity. The analysis shows that the presence of tertiary hydrogen bond acceptor groups is important for CCR2 antagonism. Fragments containing benzene ring substituted with one or more chlorine atoms show the positive effect of electron withdrawing group for favorable activity.

© 2008 Elsevier Ltd. All rights reserved.

Chemokines, also known as chemotactic cytokines, are small molecular weight (8–10 kDa) water soluble proteins consisting of 340–380 amino acid residues.^{1–3} They play an important role in the immunomodulation and host defense mechanism by attracting the cells such as monocytes, macrophages, T-cells, eosinophils, and basophils to the site of inflammation. Different chemokines produce different leukocyte responses depending on the complementarity of their chemokine receptors.^{4,5} There are 50 types of chemokines known till now and they are classified into four families viz., CC, CXC, CX3C, and XC based on their structure and function. The CC chemokines is the major family which consists of the Monocyte Chemoattractant Protein-1 (MCP-1), the most characterized protein, also known as ‘chemokine ligand CCL2’.^{6–8} The CC family consists of several CC receptors (CCR 1–10), of which CCR2 is the primary receptor for MCP-1. Studies show that MCP-1 involves in the pathophysiology of the acute or chronic inflammatory conditions such as rheumatoid arthritis, atherosclerosis, asthma, obesity, and type-2 diabetes

making CCR2 receptor as an attractive target for the drug discovery.^{9–11} A few pharma companies are working on the antagonism of CCR2 and several molecules are under phase 1 and phase 2 clinical trials (Chart 1).¹² The crystal structure of CCR2 is not yet reported. In the absence of structural information the ligand-based approaches are more valuable than structure-based methods. In the present case, however, a few studies based on modeled structure of CCR2 have been

Company	Representative molecule	Status	Disease Condition
ChemoCentryx	CCX915	Phase I IND filed	Multiple sclerosis and atherosclerosis.
Incyte and Pfizer	INCB3284	Phase II a	Rheumatoid arthritis and type 2 diabetes
Merck	MK0812	Phase II	Multiple sclerosis and pain.
Millennium Pharmaceuticals	MLN1202	Phase II	Rheumatoid arthritis, multiple sclerosis, and atherosclerosis.
Telik	MCP-1 antagonist	Preclinical	Rheumatoid arthritis, multiple sclerosis, inflammatory bowel disease, atherosclerosis, asthma, and cancer.

Chart 1. Representative CCR2 antagonists in different phases of clinical trials.

Keywords: Chemokines; CCR2 receptor; HQSAR; Molecular hologram; Indolopiperidine derivatives; Hologram fingerprint.

* Corresponding author. Tel.: +91 172 2211343; fax: +91 172 2214692; e-mail: mesophia@niper.ac.in

reported in the literature.^{13,14} The aim of the work is not only to develop a statistically significant HQSAR model but also to explore the structural and topological requirements of the molecules for CCR2 antagonism.

For the present study, we used the CCR2 receptor antagonistic activity of 35 conformationally restricted indolopiperidine analogs reported by Forbes et al.¹⁵ and Witherington et al.¹⁶ (Table 1). The biological activity was carried out using a radioligand binding displacement assay.¹³ Out of 44 reported molecules we selected 35 molecules for generating the model. Four molecules reported twice and five molecules without definite K_i values were excluded from the study. We segregated the 35 molecules in the data set into training and test set having 29 and 6 molecules, respectively. The K_i (nM) values were converted into the $-\log K_i$ (nM).

All molecular modeling studies were performed using the molecular modeling package SYBYL 7.1¹⁷ installed on a Silicon Graphics Fuel Work station. Molecules were sketched and minimized using Powell's conjugate gradient method.¹⁸ The minimum energy difference of 0.001 kcal/mol was set as a convergence criterion.

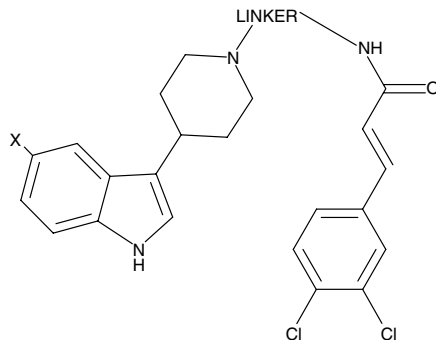
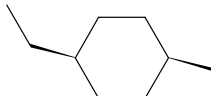
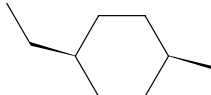
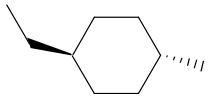
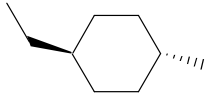
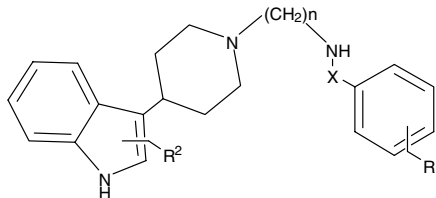
Hologram QSAR (HQSAR) is a technique which employs fragment fingerprints as predictive variables of biological activity or other structural related data. These molecular fingerprints are broken into strings at fixed interval as specified by a hologram length (HL) parameter. The hologram length determines the number of bins in the hologram into which the fragments are hashed. Each corresponding fragment SLN is then mapped to a pseudo-random integer in the range 0–231 using the CRC (cyclic redundancy check) algorithm.¹⁹ The integer generated by the CRC algorithm is unique and reproducible for each and every unique SLN string. The hashing then occurs by folding the pseudorandom integer for a particular SLN string into the bin range defined. In HQSAR, bins contain information about the number of fragments hashed into each bin. The optimal HQSAR model was derived from screening through the 12 default HL values, which were a set of 12 prime numbers ranging from 53 to 401.

HQSAR uses different parameters for model development. The parameters like atom count, hologram length and fragment distinctions²⁰ are important while generating the molecular holograms. The atom parameters enable fragment determination based on elemental atom types while the bonds and connections consider the bond orders and hybridization states within fragments, respectively. Initially, for the developing the model, we used the default parameters namely atoms (A), bonds (B), and connections (C) that gave poor r^2 (0.453) and q^2 (0.280) values. Alternatively additional parameters as hydrogen atoms (H) chirality (Ch), donor acceptor (DA) were included to develop robust models. We developed numerous models with the combination of parameters such as A/B, A/DA, B/DA, A/B/C, A/B/H, A/B/DA, A/B/C/H, A/B/H/DA, A/B/C/Ch, A/B/DA/Ch, A/B/C/H/Ch, A/B/C/Ch/DA, A/B/C/H/DA, A/B/H/DA/

Ch, A/B/D/H/Ch/DA.²¹ These models were built using the default atom count 4–7 (Table 2). The combination having atoms, bonds, chirality, and donor acceptor gave statistically significant r^2 and q^2 of 0.916 and of 0.562 values, respectively. As the second criterion for improving the statistical values, we used the atom count which refers to the minimum and maximum length of the molecular fragment. The statistical parameters obtained for a variety of models developed using A/B/Ch/DA parameters with different atom count are depicted in Table 3. A significant difference was noticed in statistical values when the model was developed with atom count 4–7 (Table 3). Further increase or decrease in the atom count reduced the overall statistical power of the model. Therefore, we selected the model developed with atom count of 4–7 with essential parameters namely atoms, bonds, donor acceptor, chirality for further analysis. It is interesting to note that in the present study all the 6 molecules of test set were predicted well by the model with a notable predictive r^2 of 0.662. The plot of actual versus predicted $-\log K_i$ (nM) of the training and test set molecules is shown in Figure 1.

The HQSAR module in SYBYL uses the color coding to show the atomic contributions to the activity. While the color codes red, red orange, and orange show the unfavorable or negative contribution to the activity, the color codes yellow, green blue, and green denote favorable, or positive contribution to the activity. The white color shows the intermediate contribution to the activity (Fig. 2).²² The molecules in the data set can be classified into four groups based on the substitutions of the functional groups. The first group contains four molecules (1–4 in Table 1), with ring as the linker group. The most active molecule 2 in this class has 5 substituted OH on the indole ring, which probably contributes for its high activity (Table 1). This may be supported by the presence of green color code between the piperidine and cyclohexane rings. The second class of molecules has variation in the amide group and contains six molecules (5–10, Table 1). And in this group, the piperidine ring probably contributes to the enhancement of activity as shown by the code green at the piperidine ring. Considering one of the active molecules 10 in this class, the presence of additional nitrogen contributes for increase in activity of the molecule. It is encoded by yellow, inferring moderate contribution to the biological activity. The third group contains seventeen molecules with the variation in the cinnamide group (13–27, 28, 29, Table 1) and in this group the two molecules (28 and 29) exhibit distinct chain lengths. This group also has the least active molecule 26 shown by red and orange color coding in the CH₂ of aliphatic chain. The indole ring contributes favorably for molecules 13, 20, 21, 23, 24, 25, 26, and 27 as pointed out by the green color in the indole ring. The fourth class of molecules has variation in the indole ring and contains eight molecules (31–38, Table 1). Substitution of 5-OH on the indole ring increases the activity as in the most active molecule 32. The same may be coded by yellow and white to show positive contributions. Overall, the activity of the molecules arises due to the presence of the piperidine ring and the active molecules, for example, 1, 2, 32, 33, 35, and 36 all have

Table 1. The data set chosen for HQSAR study, K_i values, actual and predicted $-\log K_i$ (nM) values, and residuals

<div></div>									
No.	Molecule	Linker	X	K_i (nM)	Actual $-\log K_i$ (nM)	Predicted $-\log K_i$ (nM)	Residual		
1	1		H	126	6.90	6.52	0.38		
2	2		OH	79	7.10	6.90	0.20		
3	3		H	631	6.19	6.52	−0.33		
4	4		OH	316	6.50	6.90	−0.40		
<div></div>									
No.	Molecule	X	R ¹	R ²	n	K_i (nM)	Actual $-\log K_i$ (nM)	Predicted $-\log K_i$ (nM)	Residual
5	5*	C=O	4-Ph	H	5	5400	5.26	5.34	−0.08
6	6	C=O	4-Br	H	5	7100	5.14	5.18	−0.04
7	7	C=O	3,4-diCl	H	5	5100	5.29	5.28	0.01
8	8	C(=O)CH ₂	3,4-diCl	H	5	4400	5.35	5.27	0.08
9	9	C(=O)CH ₂ CH ₂	3,4-diCl	H	5	5900	5.22	5.19	0.03
10	10	C(=O)NH	3,4-diCl	H	5	1600	5.79	5.75	0.04
11	13	<i>trans</i> C(=O)CH=CH	H	H	5	870	6.06	5.97	0.09
12	14	<i>trans</i> C(=O)CH=CH	4-Cl	H	5	520	6.28	6.15	0.13
13	15	<i>trans</i> C(=O)CH=CH	3-Cl	H	5	560	6.25	6.19	0.06
14	16	<i>trans</i> C(=O)CH=CH	2-Cl	H	5	4400	5.35	5.80	−0.45
15	17*	<i>trans</i> C(=O)CH=CH	4-Br	H	5	350	6.45	6.15	0.30
16	18*	<i>trans</i> C(=O)CH=CH	4-I	H	5	460	6.33	6.03	0.30
17	19	<i>trans</i> C(=O)CH=CH	3-CF ₃	H	5	790	6.10	6.06	0.04
18	20	<i>trans</i> C(=O)CH=CH	4-Me	H	5	550	6.25	6.10	0.15
19	21	<i>trans</i> C(=O)CH=CH	3-Me	H	5	790	6.10	6.09	0.01
20	22*	<i>trans</i> C(=O)CH=CH	4-Ph	H	5	1450	5.83	5.85	−0.02
21	23	<i>trans</i> C(=O)CH=CH	4-But	H	5	1700	5.76	5.88	−0.12
22	24	<i>trans</i> C(=O)CH=CH	4-NMe ₂	H	5	1200	5.92	5.99	−0.07
23	25	<i>trans</i> C(=O)CH=CH	4-OH	H	5	6300	5.20	5.21	−0.01

Line missing

24	26	<i>trans</i> C(=O)CH=CH	4-NHAc	H	5	12,900	4.88	4.80	0.08
25	27	<i>trans</i> C(=O)CH=CH	4-CN	H	5	2800	5.55	5.66	−0.11

Table 1 (continued)

No.	Molecule	X	R ¹	R ²	n	K _i (nM)	Actual −log K _i (nM)	Predicted −log K _i (nM)	Residual
26	28	<i>trans</i> C(=O)CH=CH	3,4-diCl	H	3	2500	5.60	5.46	0.14
27	29*	<i>trans</i> C(=O)CH=CH	3,4-diCl	H	4	660	6.18	6.65	−0.47
28	31	<i>trans</i> C(=O)CH=CH	3,4-diCl	H	5	420	6.37	6.52	−0.15
29	32	<i>trans</i> C(=O)CH=CH	3,4-diCl	5-OH	5	50	7.30	6.91	0.39

Line missing

Table 2. Statistical parameters obtained for different HQSAR parameters

Model	Fragment distinction	q ² (LOO)	r ² ncv	SE	BHL	Component
1	A/B	0.242	0.394	0.507	83	1
2	A/DA	0.255	0.437	0.489	401	1
3	B/DA	0.422	0.759	0.333	97	3
4	A/B/C	0.280	0.453	0.482	199	1
5	A/B/H	0.421	0.78	0.324	71	4
6	A/B/DA	0.437	0.876	0.249	53	5
7	A/B/C/H	0.355	0.734	0.349	199	3
8	A/B/H/DA	0.464	0.779	0.325	53	4
9	A/B/C/Ch	0.290	0.459	0.479	199	1
10	A/B/DA/Ch	0.562	0.916	0.209	53	6
11	A/B/C/H/Ch	0.406	0.721	0.358	199	3
12	A/B/C/Ch/DA	0.345	0.719	0.359	83	3
13	A/B/C/H/DA	0.400	0.789	0.318	199	4
14	A/B/H/DA/Ch	0.440	0.803	0.307	53	4
15	A/B/DA/H/Ch/DA	0.378	0.781	0.323	151	4

The best model is highlighted in bold font.

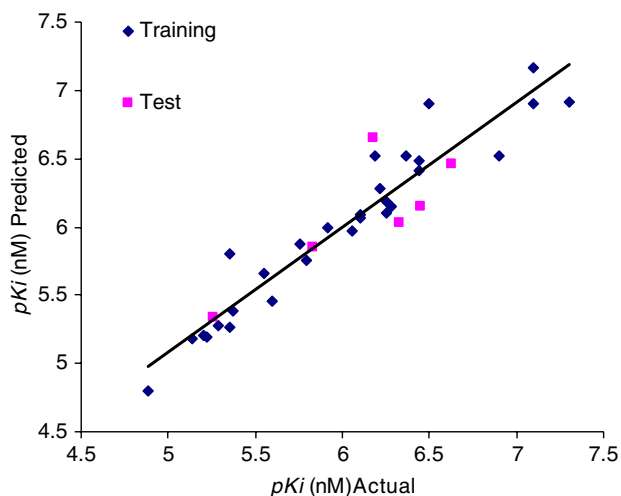
Table 3. Statistical parameters obtained for model 10 with different atom count

Atom count	q ² (LOO)	r ² ncv	SE	BHL	Component
1–4	0.295	0.68	0.383	83	3
2–5	0.320	0.71	0.364	257	3
3–6	0.341	0.604	0.418	59	2
4–7	0.562	0.916	0.209	53	6
5–8	0.362	0.74	0.345	97	3
6–9	0.374	0.702	0.37	83	3
7–10	0.406	0.684	0.381	71	3

The model chosen for analysis is highlighted in bold fonts.

contributions from the piperidine ring as coded by green. Furthermore, the indole ring shows partial contributions to the activity as shown by the white color code. Finally the red and orange codes may be indicative of negative contributors to the C₅ chain. This is reflected by molecules **6**, **7**, **9**, **16**, **25**, and **26**.

In HQSAR the fragment is useful in predicting the variability in biological activity. We analyzed the fragment produced by HQSAR which aided us to throw light on some of the important features as highlighted below. The final HQSAR model produced hundreds of fragments. Although direct correlation between the activity and all the produced fragments may not be possible, yet fragments indicated useful hints toward improvement of the activity. Analysis of the fragments and their contributions shows that the presence of fragments pos-

**Figure 1.** Plot of actual versus predicted −log K_i (nM) values of the training and test set molecules. The training set and test set molecules are shown in blue (diamond) and pink (square) spots, respectively.

sessing positive values contributes favorably to the activity. Similarly fragments possessing negative values contribute unfavorably to the activity. For example, the fragment F1 (Fig. 3) having positive coefficient value of 0.045 has a tertiary hydrogen bond acceptor. This fragment is present in all the molecules of the data set and shows one may prefer tertiary hydrogen bond acceptor group while designing new scaffolds for

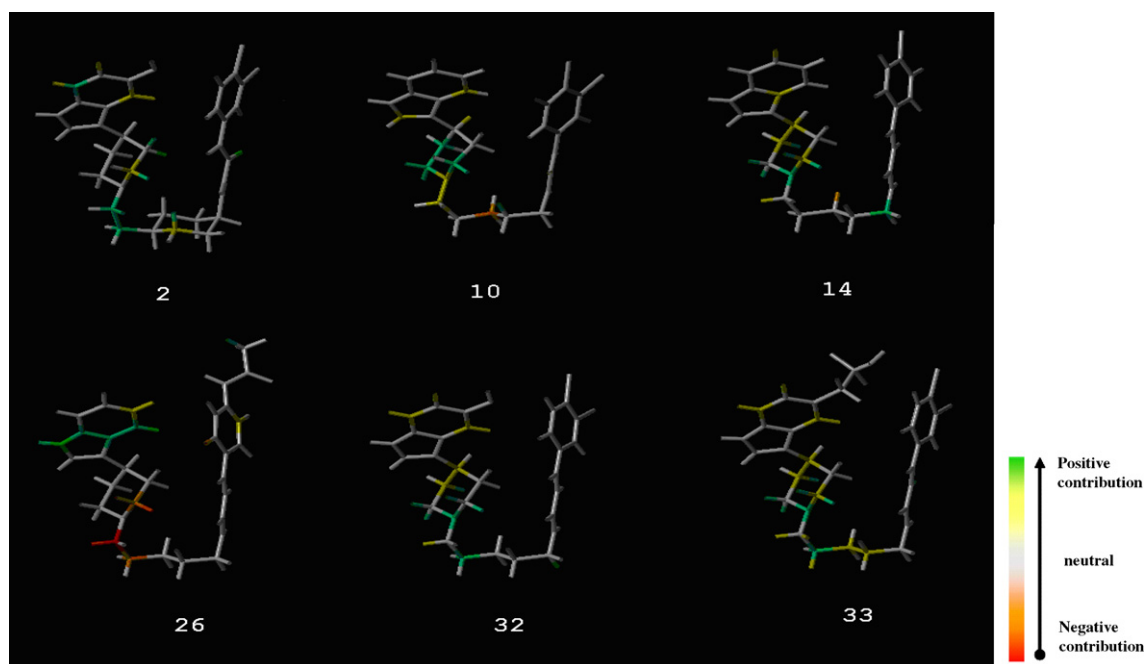


Figure 2. Contribution map obtained for a few molecules by HQSAR analysis.

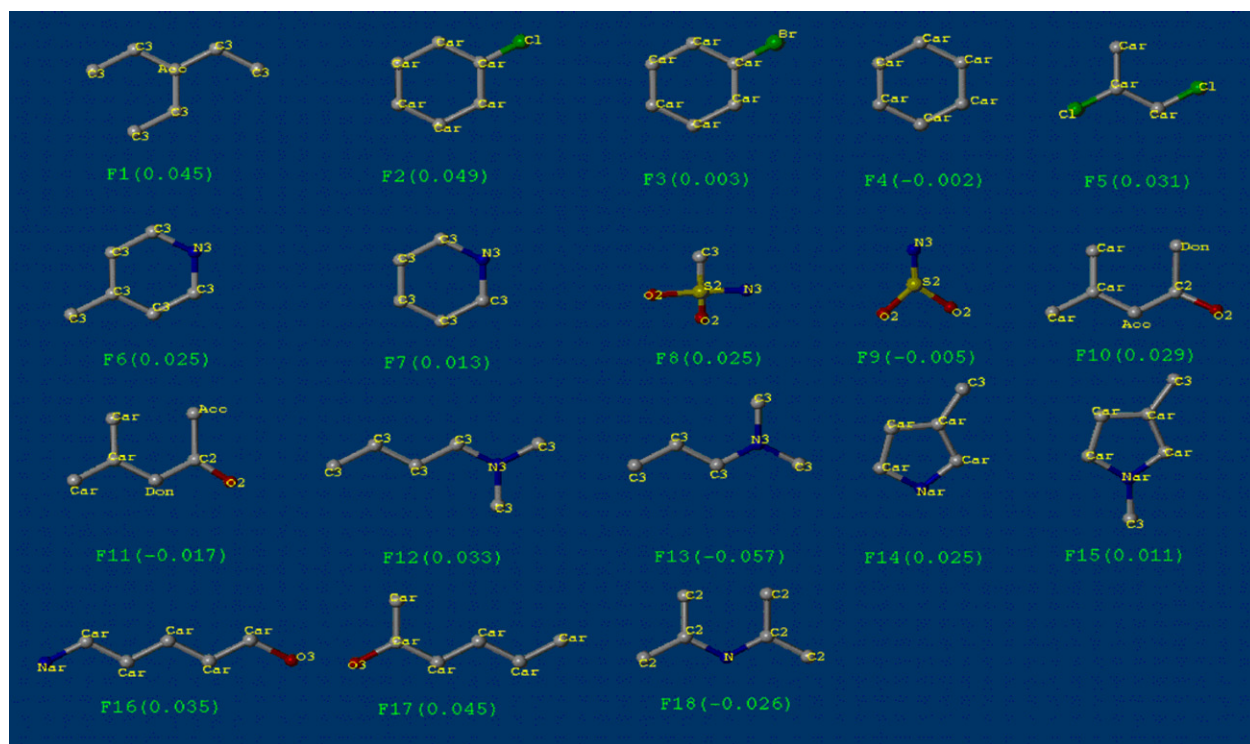


Figure 3. A few fragments showing positive and negative contributions toward CCR2 antagonism.

CCR2 antagonism, as found in all the molecules of the data set. This point is supported by the literature study that the tertiary acceptor like nitrogen is identified as an important fragment for CCR2 antagonism in the Roche, Takeda's, and Smithkline Beecham compounds.^{13,23} This point is further sustained by the recent 3D-QSAR CoMFA study of Dasse et al. wherein they have pointed out that all their newly designed molecules possess tertiary nitrogen acceptor group highlighting its importance toward CCR2 antagonism.²⁴

On consideration of the three fragments F2, F3, and F4 having benzene ring with mono substituted chlorine (0.049), mono substituted bromine (0.003), and unsubstituted ring (−0.002), respectively, a decline in the coefficient values may be noticed. This emphasizes the effect of electron withdrawing group for favorable activity. The fragment F2 is present in the molecule **15** ($K_i = 560$ nM) which shows good activity. The unsubstituted ring fragment F4 is present in the molecule **13** ($K_i = 870$ nM) which is having lesser activity than

molecule **15**. The bromine containing fragment F3 is seen in the molecule **6** ($K_i = 7100$ nM) which is the least active molecule among the three. Despite having the bromine containing fragment which displays medium coefficient value, the molecule **6** illustrates the least activity among the three. This may be due to the reason that, other fragments presumably have an influence on the activity of **6**. The fragment F5 consists of two chlorine atoms displaying higher positive value as the coefficient and further highlights the effect of more chlorine substitutions on the activity. It is interesting to note many of the active molecules contain this fragment.

Analysis of the two fragments F6 (0.025) and F7 (0.013) showed F6 has piperidine with carbon attached to it where as F7 does not have any substitution on the ring. The coefficient value for F7 shows, the attached carbon on piperidine moiety may play a positive role in increasing the activity. In F8 (0.025) and F9 (−0.005), the sulfur atom plays a role, the hexa-valent sulfur atom present in F8 (0.025) in methyl sulfonamide group contributes positively while penta-valent sulfur present in F9 contributes negatively. This shows the influence of multi valency of sulfur atoms on activity as seen in the molecule **33** ($K_i = 79$). It is interesting to note that, in F10 (0.029), the three substitutions viz., acceptor group, Zaccany (Oxygen or Acceptor), and Donor are arranged consecutively so that the electrons delocalization is effected. This particular way of arrangement causing electrons delocalization seems to be a favorable property for the increase in activity. It is interesting to note that when the three groups are arranged in different order, then the contribution to the activity decreases as shown by the F11 (−0.017). By looking at F12 (0.033), F13 (−0.057), we can say the aliphatic chain length increases the activity of the molecules because of the increase in the electron density on the nitrogen of piperidine ring as seen in **29** and **28** ($K_i = 2500$ and 660). The fragment F14 (0.025) is having mono substitution and in F15 (0.011) the substitution is on the nitrogen atom and it increases the electron density on nitrogen and thus decreases the activity as in **37** ($K_i = 4200$). The F16 (0.035) exhibits resonance effect that contributes favorably to the activity. In this fragment nitrogen has lone pair of electrons, the aromatic carbons have delocalized electrons, and the oxygen has lone pair of electron, and all these three substitutions cause resonance effect in the molecule. This fragment is present in the most active molecule **32** ($K_i = 50$). Further, we can note that when the donor group is present at the end of fragment as the one in F17 (0.045) the resonance effect further increases and so the contribution. While the highest active molecule contains the fragments like F1, F2, F6, F12, F16, and F17 that contribute positively, the least active molecule **26** ($K_i = 12,900$) has fragments that contribute negatively for the activity.

CCR2 is the major family of chemokine receptors which are implicated in the pathophysiology of the acute or chronic inflammatory conditions such as rheumatoid arthritis, atherosclerosis, asthma, obesity, and type-2 diabetes. HQSAR model was developed for a set of

indolopiperidine derivatives. The model 10 developed using the combination of parameters having atoms, bonds, chirality, donor acceptor, and atom count 4–7 gave statistically significant r^2 and q^2 of 0.916 and of 0.562 values, respectively. The analysis of contribution map shows the activity of the molecules arises due to the presence of the piperidine ring. For example, the molecules **1**, **2**, **32**, **33**, **35**, and **36** all have contributions from the piperidine ring as encoded by green. The less active molecules have the negative contributions from C₅ chain as reflected by the presence of red and orange codes in the molecules **6**, **7**, **9**, **16**, **25**, and **26** at C₅ chain. Analysis of molecular fragments throws light on essential structural and topological features of indolopiperidine derivatives for antagonist activity. The model so generated is also consistent with the literature support that the tertiary acceptor like nitrogen is identified as an important fragment for CCR2 antagonism.

Through HQSAR analysis we noted the following for the improvement of CCR2 antagonist activity.

1. Presence of tertiary acceptor group.
2. Presence of one or more chlorines, substituted at 3, 4, or 5 position of benzene.
3. Effect of resonance in 5 substituted indole ring.
4. Aliphatic chain length up to 5 increases the activity of the molecules due to increase in the electron density on the nitrogen of the piperidine ring.

Overall, the information gained from our analysis will be useful in guiding the chemists in obtaining novel and more active molecules for CCR2.

References and notes

1. Lihu, Y.; Changyou, Z.; Liangqin, G.; Gregori, M.; Gabor, B.; Alexander, P.; William, H. P.; Sander, G. M.; Malcolm, M.; Pasquale, P. V.; Hans, Z.; Julia, M. A.; Shefali, G.; William, A. H.; Margaret, A. C.; Springer, M. S. *Bioorg. Med. Chem. Lett.* **2006**, *16*, 3735.
2. Gabor, B.; Gregori, J. M.; Shankaran, K.; Deodial, G.; Alexander, P.; William, H. P.; Malcom, M.; Pasquale, P. V.; Margaret, A. C.; Yang, L. *Bioorg. Med. Chem. Lett.* **2006**, *16*, 4715.
3. Anthony, B. P.; Dehua, H.; Rowena, V. C.; John, H. H.; Mary, S.; Julia, M. A.; Pasquale, P. V.; Sima, R. P.; Thomas, W.; Julie, A. D.; Jean, M. V. *Bioorg. Med. Chem. Lett.* **2007**, *17*, 807.
4. Tara, M.; Frank, D.; Bettina, E.; Sunil, B.; Irene, P.; Deborah, M.; Mary, M.; Gabe, S. W.; Jean, M. L.; John, D.; David, M.; Wilhelm, R.; Jarnagin, K. *J. Biolog. Chem.* **2000**, *275*, 25562.
5. Tsou, C. L.; Peters, W.; Si, Y.; Slaymaker, S.; Aslanian, A. M.; Weisberg, S. P.; Mack, M.; Charo, I. F. *J. Clin. Inv.* **2007**, *117*, 902.
6. Israel, F. C.; Ranshoff, R. M. *N. Engl. J. Med.* **2006**, *354*, 610.
7. Jason, G. K.; Alan, W. F.; Andy, J. B.; Huw, D.; Stone, M. A. *Bioorg. Med. Chem. Lett.* **2004**, *14*, 405.
8. Changyou, Z.; Liangqin, G.; William, H. P.; Sander, G. M.; Malcolm, M.; Pasquale, P. V.; Hans, Z.; Margaret, A. C.; Springer, M. S.; Yang, L. *Bioorg. Med. Chem. Lett.* **2007**, *17*, 309.

9. Minoru, I.; Tatsuki, S.; Ken ichiro, K.; Christine, M. T.; Wilna, J. M.; Takaharu, T.; Masaki, S.; Michele, M. R. W.; Daniel, C.; Chung, M. S.; Shinsuke, Y.; Hiroko, T.; Takuya, M.; Takahiko, H.; Jonathan, G.; Doug, B.; John, S.; Peter, L. M.; Yoshinori, K.; Endo, N. *Bioorg. Med. Chem. Lett.* **2004**, *14*, 5407.
10. Wilna, J. M. A.; Ken ichiro, K.; Michele, M. R. W.; Tatsuki, S.; Minoru, I.; Masaki, S.; Takaharu, T.; Noriaki, E.; Yumiko, M.; Takahiko, H.; Hiroko, T.; Takuya, M.; Jonathan, G.; Doug, B. A. J. S.; Yoshinori, K.; Peter, L. M.; Christine, M. T. *Bioorg. Med. Chem. Lett.* **2004**, *14*, 5413.
11. Stuart, P. W.; Deborah, H.; Reid, H.; Jacob, L.; Sarah, S.; Kris, V.; Israel, C.; Rudolph, L. L., Jr.; Alan, W. F. *J. Clin. Investig.* **2006**, *116*, 115.
12. Sannes, L. <http://www.pharmaweek.com>.
13. Berkhout, T. A.; Blaney, F. E.; Bridges, A. M.; Cooper, D. G.; Forbes, I. T.; Gribble, A. D.; Groot, P. H. E.; Hardy, A.; Ife, R. J.; Kaur, R.; Moores, K. E.; Shillito, H.; Willetts, J.; Witherington, J. *J. Med. Chem.* **2003**, *46*, 4070.
14. Marshall, T. G.; Lee, R. E.; Marshall, F. E. *Theor. Biol. Med. Model.* **2006**, *10*, 3.
15. Forbes, I. T.; Cooper, D. G.; Dodds, E. K.; Hickey, D. M.; Ife, R. J.; Meeson, M.; Stockley, M.; Berkhout, T. A.; Gohil, J.; Groot, P. H. *Bioorg. Med. Chem. Lett.* **2000**, *10*, 1803.
16. Witherington, J.; Bordas, V.; Cooper, D. G.; Forbes, I. T.; Gribble, A. D.; Ife, R. J.; Berkhout, T.; Gohil, J.; Groot, P. H. *Bioorg. Med. Chem. Lett.* **2001**, *11*, 2177.
17. SYBYL7.1, Tripos Associate Inc.; 1699, S. Hanley Rd., St. Louis, MO 631444, USA.
18. Powell, M. J. D. *Math. Prog.* **1977**, *12*, 241.
19. Lowis, D. R. *Tripos Tech. Notes* **1997**, *1*, 1.
20. Carlos, R. R.; Terrence, M. F.; Clayton, S.; James, H. M.; Cohen, F. E. *Bioorg. Med. Chem. Lett.* **2002**, *12*, 1537.
21. Castillo, M. S.; Guido, R. V. C.; Andricopulo, A. D. *Lett. Drug Des. Discov.* **2007**, *4*, 106.
22. Honorio, K. M.; Garratt, R. C.; Andricopulo, A. D. *Bioorg. Med. Chem. Lett.* **2005**, *15*, 3119.
23. Baba, M.; Nishimura, O.; Kanzaki, N.; Okamoto, M.; Sawada, H.; Iizawa, Y.; Shiraishi, M.; Aramaki, Y.; Okonogi, K.; Ogawa, Y. *Nat. Acad. Sci.* **1999**, *96*, 5698.
24. Dasse, O. A.; Evans, J. L.; Zhai, H. X.; Zou, D.; Kintigh, J. T.; Chan, F.; Hamilton, K.; Hill, E.; Eckman, J. B.; Higgins, P. J.; Volosov, A.; Collart, P.; Nicolas, J. M.; Kondrui, R. K.; Schwartz, C. E. *Lett. Drug Des. Discov.* **2007**, *4*, 263.